Available online at www.sciencedirect.com
SCIENCE DIRECT®
Journal of the European Ceramic Society 25 (2005) 543–547
www.elsevier.com/locate/jeurceramsoc

Influence of a finite notch root radius on fracture toughness

T. Fett*

Forschungszentrum Karlsruhe, Institut für Materialforschung II, Hermann von Helmoholtz-Platz 1, Postfach 3640, D-76021 Karlsruhe, Germany

Received 6 July 2003; received in revised form 19 January 2004; accepted 25 January 2004

Available online 15 June 2004

Abstract

The validity of fracture toughness data from tests with V-notched bending bars depends in the notch root radius and the presence of an *R*-curve behaviour. In a theoretical study it is shown how the notch radius affects the formally computed conventional toughnesses. These are computed under the assumption that the introduced notch with a small crack at the notch root acts as a long crack of the same total size and, in a stronger simplification, that the crack length is identical with the depth of the notch.

Keywords: Crack tip toughness; Fracture toughness; Notch effect; *R*-curve; Testing

1. Introduction

Most investigations of fracture toughness deal with cracks starting from narrow notches. These are introduced in test specimens by thin saw cuts or produced with the razor blade procedure as proposed by Nishida et al.[1] and successfully applied by Kübler.[2] If a_0 is the depth of the notch and ℓ the length of an edge crack propagating from the notch root (for the geometric data see Fig. 1a), the stress intensity factor commonly, but incorrectly is computed as the stress intensity factor for a crack of total length $a = a_0 + \ell$

$$K^* = \sigma_{\text{bend}} \sqrt{\pi(a_0 + \ell)}\, F_{\text{bend}} \left(\frac{a}{W}\right) \tag{1}$$

where F_{bend} is the geometric function for an edge crack of length $a = a_0 + \ell$ in a specimen of width W under the applied load, here, for instance, under bending load. The geometric function is available from fracture mechanics handbooks. The formally computed "apparent stress intensity factor" K^* given by Eq. (1) is the correct value only in cases where the crack length ℓ is clearly larger than the radius of the notch. In the first crack extension phase where the crack length ℓ is comparable to R, Eq. (1) does not represent the correct stress intensity factor value.

In fracture toughness tests the stress intensity factor is often computed with the notch depth a_0 as the crack length. This is necessary in all cases where the crack length at failure cannot be identified on the fracture surface. This value may be denoted here by $\hat{K}$ with

$$\hat{K} = \sigma_{\text{bend,max}} \sqrt{\pi a_0}\, F_{\text{bend}} \left(\frac{a_0}{W}\right) \tag{2}$$

It is clear that in the presence of a strong *R*-curve behaviour with an extended stable crack growth phase before final fracture, Eq. (2) badly describes the fracture toughness, even if notch effects are negligible. It is the aim of this contribution to show the influence of the notch root radius and *R*-curve on the formally computed toughnesses according to Eqs. (1) and (2).

2. Notch effect and *R*-curve

To examine the case of a material with *R*-curve, the fracture mechanics problem of a small crack in front of a finite notch has to be considered. In the special case of an edge crack ahead of a slender notch with R being small compared to the crack length and the other specimen dimensions, the true stress intensity factor K is given by[3]

$$\frac{K}{K^*} = \tanh\left(2.243\sqrt{\frac{\ell}{R}}\right) \tag{3}$$

This relation is shown in Fig. 2 as the dashed curve. If a semi-elliptical crack is assumed (for the geometric data see

* Tel.: +49-7247-82-2347; fax: +49-7247-82-5070.
E-mail address: theo.fett@imf.fzk.de (T. Fett).

0955-2219/$ – see front matter © 2004 Elsevier Ltd. All rights reserved.
doi:10.1016/j.jeurceramsoc.2004.01.010

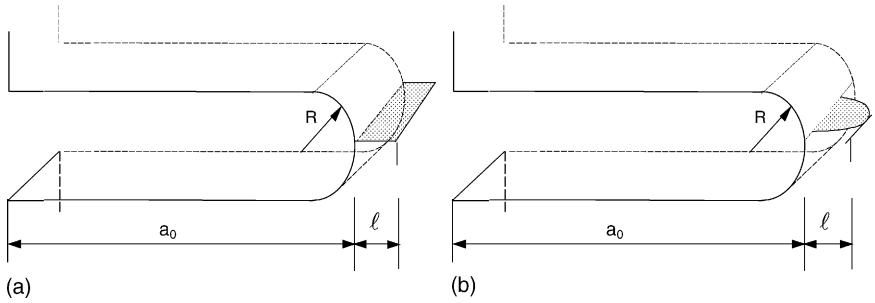

Fig. 1. Cracks in front of a narrow notch: (a) edge crack and (b) semi-elliptical crack.

Fig. 1b), then as shown in[4]

$$\frac{K}{K^*} \cong \tanh\left(2.243 g\left(\frac{\ell}{R}\right)\sqrt{\frac{\ell}{R}}\right) \tag{4}$$

with

$$g\left(\frac{\ell}{R}\right) \cong \frac{2}{3} + 0.178\left(1 - \exp\left(-1.64\frac{\ell}{R}\right)\right) \tag{5}$$

In Fig. 2 this relation is shown by the solid curve. From the curves of Fig. 2a, it is clearly visible that the true stress intensity factor is significantly lower than the formally computed values of K^*, irrespective of the special crack shape. On the other hand, it can be concluded that notch effects are without importance for $\ell > 1.5R$. For the following numerical evaluations, Eq. (3) will be used.

Replacing of K^* in Eq. (3) by this formally computed "apparent fracture toughness" yields

$$K \cong \hat{K}\sqrt{\frac{a_0+\ell}{a_0}}\frac{F(a/W)}{F(a_0/W)}\tanh\left(2.243\sqrt{\frac{\ell}{R}}\right) \tag{6}$$

Sometimes, this relation was successfully used for a fracture toughness evaluation,[2,5–7] where the rough approximation

$$\sqrt{\frac{a_0+\ell}{a_0}}\frac{F(a/W)}{F(a_0/W)} \approx 1 \Rightarrow\ K \approx \hat{K}\tanh\left(2.243\sqrt{\frac{\ell}{R}}\right) \tag{7}$$

was made, which is applicable for $\ell \ll a_0$ at least. Damani et al.[5,6] further assumed ℓ to be proportional to the size of defects at the notch root caused by notch preparation or to the mean grain size, since grain boundaries may act as crack-like defects. Errors in toughness determination are unavoidable, at least in the case of a significant stable crack extension before failure, as expected for materials with a pronounced R-curve behaviour. In this case, the maximum load indicated by the solid circle in the load versus displacement curve of Fig. 2b is commonly introduced in Eq. (2), although the load versus displacement plot shows a clear deviation from the initial straight line, starting at the open circle.

In a material with an R-curve effect, the externally applied stress intensity factor K_{appl} and the intrinsic shielding stress intensity factor have to be superimposed in order to obtain the total stress intensity factor K_{total}

$$K_{total} = K_{appl} + K_{sh} \tag{8}$$

which governs the crack tip stress field. Fig. 3a represents these stress intensity factor contributions.

Stable crack propagation occurs under the condition of the total stress intensity factor equalling the so-called crack tip toughness K_{I0}

$$K_{total} = K_{I0} \tag{9}$$

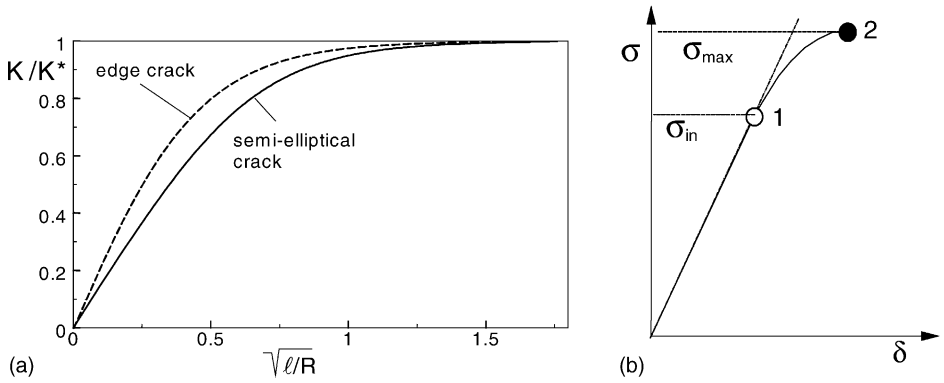

Fig. 2. (a) Ratio of true stress intensity factor K and formally computed stress intensity factor K^* as a function of ℓ/R, (b) stresses in a fracture toughness test, σ_{in} = stress at the first deviation from the initial straight line of the load vs. displacement plot, σ_{max} = stress at failure.

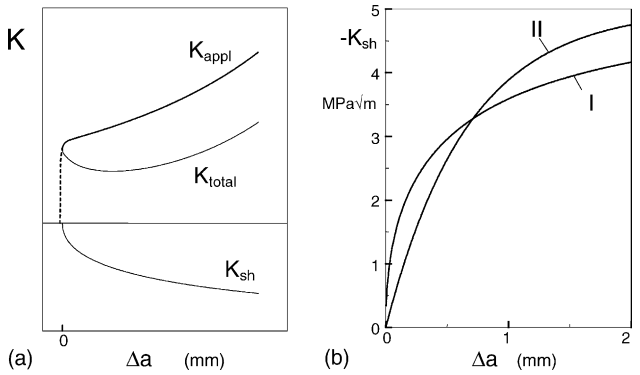

Fig. 3. (a) Total stress intensity factor obtained by superposition of the applied and the shielding stress intensity factors according to Eq. (8), (b) shielding stress intensity factors according to Eq. (10), "*R*-curve I" and Eq. (13), "*R*-curve II".

The influence of the notch effect on the *R*-curve in terms of $K^*_{\mathrm{appl}} = f(\Delta a)$ or $K^*_{\mathrm{appl}} = f(\Delta \ell)$, here denoted as the "apparent *R*-curve", can then be outlined in the following way.

In order to study the influence of a notch on the *R*-curve behaviour, two different types of shielding stress intensity factor are chosen. A "steep" *R*-curve behaviour may be modelled by

$$K_{\mathrm{sh}} = K_{\mathrm{sh,max}}[1 - \exp(-\lambda\sqrt{\Delta a})] \tag{10}$$

This relation, denoted as *R*-curve I, interpolates one limit case for small crack extensions

$$K_{\mathrm{sh}} \propto \sqrt{\Delta a}, \quad \text{for } \Delta a \to 0 \tag{11}$$

and the saturation behaviour

$$K_{\mathrm{sh}} \to K_{\mathrm{sh,max}}, \quad \text{for } \Delta a \to \infty \tag{12}$$

As a second possibility an initially linear *R*-curve may be chosen as

$$K_{\mathrm{sh}} = K_{\mathrm{sh,max}}[1 - \exp(-\beta \Delta a)] \tag{13}$$

denoted as *R*-curve II, which interpolates a second limit case for small crack extensions

$$K_{\mathrm{sh}} \propto \Delta a, \quad \text{for } \Delta a \to 0$$

and again $K_{\mathrm{sh}} = K_{\mathrm{sh,max}}$ for large crack extension.

The curves related to the parameters of $\lambda = 40\,\mathrm{m}^{1/2}$, $\beta = 1500\,\mathrm{m}^{-1}$, and $K_{\mathrm{sh,max}} = -5\,\mathrm{MPa\,m}^{1/2}$ are shown in Fig. 3b. As realistic crack/specimen dimensions, $W = 4$ mm and $a_0 = 2$ mm were chosen for the numerical computations. The crack tip toughness was assumed to be $K_{\mathrm{I0}} = 2.4\,\mathrm{MPa\,m}^{1/2}$ as found in[8] for alumina.

The initial crack size ℓ_0 can be estimated by comparing the crack tip toughness K_{I0} obtained from the near-tip crack opening displacement field of a grown crack with the result of strain-gauge-equipped notched bending bars.[8] Depending on the specially assumed crack type, values in the order of $\ell_0 = 2$–$5\,\mu$m were found for alumina.

3. Crack extension behaviour

The influence of the notch root radius on the total stress intensity factor is shown in Fig. 4 for an initial crack size of $\ell_0 = 2\,\mu$m and the two types of *R*-curve. Since for "*R*-curve I" an intersection between K_{total} and K_{I0} is obtained for $R < 18\,\mu$m only, this critical radius denoted as R_{c} (introduced in Fig. 4a and b as the dashed curves) is a limit for reaching stable crack extension. If $R > R_{\mathrm{c}}$, unstable crack extension must occur when $K_{\mathrm{total}} = K_{\mathrm{I0}}$ is reached for the first time. For $R < R_{\mathrm{c}}$, a stable phase during crack propagation must occur.

In the case of *R*-curve II, the limit radius is about $R_{\mathrm{c}} = 10\,\mu$m. Fig. 4c shows K_{total} for fixed $R = 16\,\mu$m and various initial crack lengths ℓ_0.

Details of the crack extension phases are revealed in Fig. 5 for a notch radius of 8 μm and an initial crack size of $\ell_0 = 2\,\mu$m. A crack of length ℓ_0 at a notch starts to propagate, if the condition $K_{\mathrm{total}} = K_{\mathrm{I0}}$ is fulfilled for the first time. Since K_{total} increases with increasing crack length, spontaneous

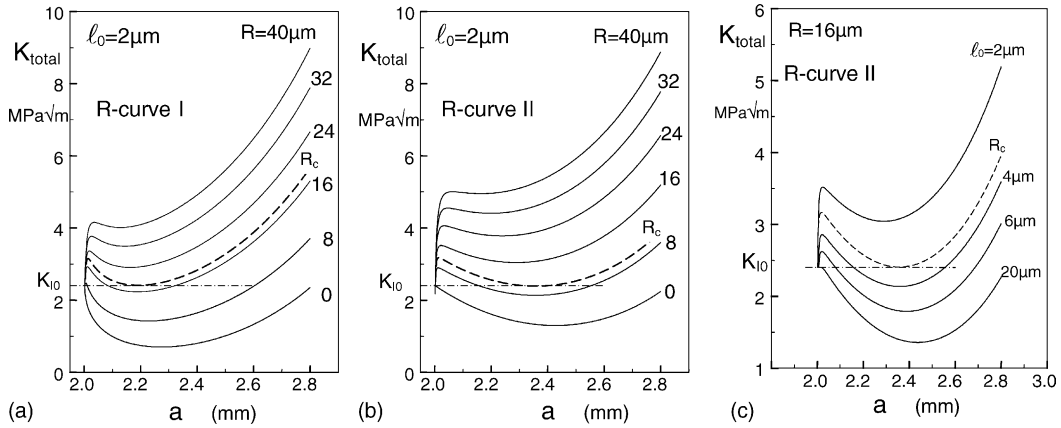

Fig. 4. Influence of the notch radius *R* and the initial crack length ℓ_0 on the total stress intensity factor (computed for $K_{\mathrm{sh,max}} = -5\,\mathrm{MPa\,m}^{1/2}$).

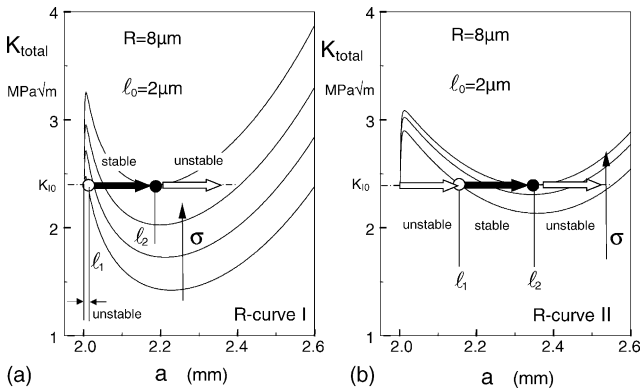

Fig. 5. Crack development for an intermediate notch radius of $R = 8\,\mu m$.

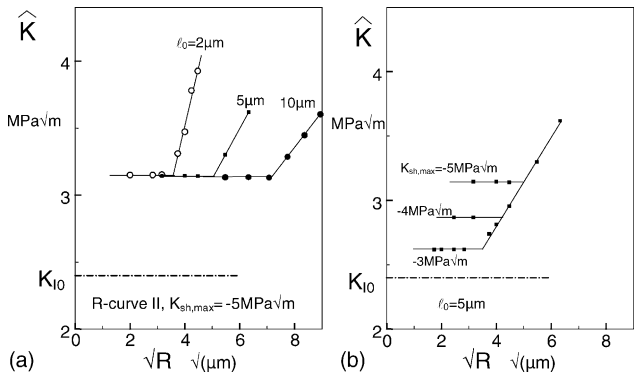

Fig. 7. Influence of initial crack length ℓ_0 and the maximum shielding stress intensity factor on conventionally determined fracture toughness.

crack extension must occur up to a crack length ℓ_1, at which $K_{total} = K_{I0}$ is fulfilled for the second time. This condition is found after 30 μm crack extension in the case of the steep *R*-curve I and 200 μm for *R*-curve II. The unstable crack extension phase is followed by stable crack propagation under increasing externally applied load. At crack length ℓ_2, the horizontal tangent at the $K_{total}(a)$-curve becomes identical with the horizontal line K_{I0} = constant. For *R*-curve I, it holds $\ell_2 \approx 200\,\mu m$ and for *R*-curve II $\ell_2 \approx 350\,\mu m$. From Fig. 5, it can be concluded that the crack length at failure, ℓ_2, is significantly larger than the initial crack length ℓ_0.

In Fig. 6 the effect of the relative notch root radius R/ℓ_0 on the apparent fracture toughness is shown. Fig. 6a illustrates the two quantities K^* and $\hat{K}$ in the absence of any *R*-curve. Whereas K^* tends to K_{I0} for $R/\ell_0 \to 0$, $\hat{K}$ tends to 0. In the presence of an *R*-curve behaviour, Fig. 6b and c, the curve for large R/ℓ_0 coincides with the curve of Fig. 6a down to a certain characteristic value of R/ℓ_0, denoted as R_c/ℓ_0. For smaller R/ℓ_0, the apparent fracture toughness reaches a saturation value.

The influences of the initial crack size and the maximum shielding stress intensity factor on the apparent fracture toughness $\hat{K}$ and the critical notch root radius R_c are represented in Figs. 7 and 8. The characteristic notch radius increases with increasing initial crack length ℓ_0 and the

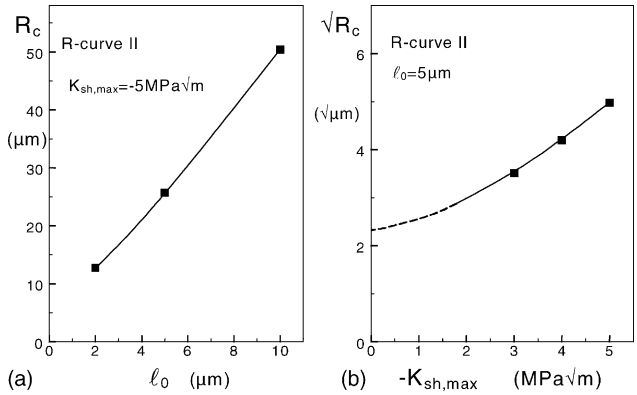

Fig. 8. Influence of initial crack size ℓ_0 and the maximum shielding stress intensity factor on critical notch root radius (computed for *R*-curve II).

apparent fracture toughness $\hat{K}$ increases with an increasing maximum shielding term. In the papers of Damani et al.[5,6] a direct correlation between the critical notch radius and the grain size was proposed. A more indirect interrelation to the grain size is obvious also from the computations made in this contribution. Fig. 7b shows that for a fixed initial crack size ℓ_0 the critical notch radius R_c increases with increasing maximum shielding stress. Since the bridging effects in

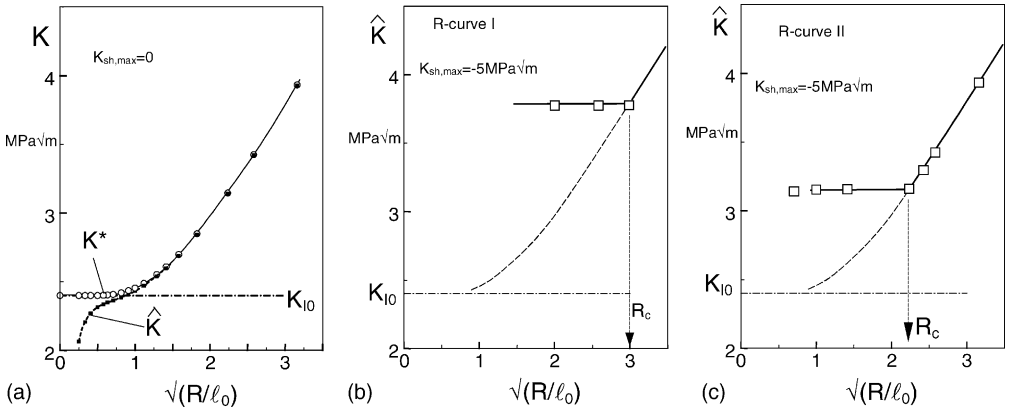

Fig. 6. Apparent toughness, computed for $R = 16\,\mu m$ and varying ℓ_0.

the crack wake, responsible for the *R*-curve behaviour in coarse-grained ceramics, increase with increasing grain size, a dependency between grain size and critical notch radius has to be expected.

4. Conclusions

As the main results, the following conclusions may be drawn for a material with rising *R*-curve:

- For a large notch root radius $R > R_c$, only spontaneous crack extension is possible;
- For a small radius $R < R_c$, crack propagation consists of stable and unstable crack extension phases with instability occurring after crack extension in the order of several 100 μm;
- The characteristic notch radius, below which a constant apparent toughness occurs, increases with increasing initial crack length ℓ_0;
- The apparent fracture toughness $\hat{K}$ increases with an increasing maximum shielding term;
- An interrelation between the characteristic notch radius R_c and the grain size exists, since the *R*-curve effect in coarse-grained ceramics increases with increasing grain size.

It can be concluded from Fig. 7a that the apparent stress intensity factor $\hat{K}$ equals the correct toughness if the measured data are located on the plateau value. This value is independent of the initial crack size l_φ and of the notch root radius *R*. It is necessary for the practical determination of toughness data to vary the notch radius and to determine the value of the plateau. If this value cannot be reached (e.g. for very fine-grained materials) the experimentally obtained apparent stress intensity factor at least gives an upper limit of the true toughness.

Acknowledgements

Financial support by the Deutsche Forschungsgemeinschaft within the SFB 483 is gratefully acknowledged.

References

1. Nishida, T., Pezzotti, G., Mangialardi, T. and Paolini, A. E., Fracture mechanics evaluation of ceramics by stable crack propagation in bend bar specimens. In *Fracture Mechanics of Ceramics, Vol 11*, ed. R. C. Bradt, D. P. H. Hasselman, D. Munz, M. Sakai and V. Y. Shevchenko. 1996, pp. 107–114.
2. Kübler, J., Fracture toughness using the SEVNB method: preliminary results. *Ceram. Eng. Sci. Proc.* 1997, **18**, 155–162.
3. Fett, T. and Munz, D., *Stress Intensity Factors and Weight Functions*. Computational Mechanics Publications, Southampton, 1997.
4. Fett, T., Estimated stress intensity factors for semi-elliptical cracks in front of narrow circular notches. *Eng. Fract. Mech.* 1999, **64**, S.357–S.362.
5. Damani, R., Gstrein, R. and Danzer, R., Critical notch-root radius effect in SENB-S fracture toughness testing. *J. Eur. Ceram. Soc.* 1996, **16**, 695–702.
6. Damani, R. J., Schuster, C. and Danzer, R., Polished notch modification of SENB-S fracture toughness testing. *J. Eur. Ceram. Soc.* 1997, **17**, 1685–1689.
7. Rudolph, E., contribution to [2].
8. Kounga, A. B., Yousef, S. G., Fett, T. and Rödel, J., Crack tip toughness of coarse-grained alumina. *J. Mater. Sci. Lett.*, in press.